JOURNAL OF THERMOPHYSICS AND HEAT TRANSFER
Vol. 21, No. 1, January–March 2007

Technical Notes

TECHNICAL NOTES are short manuscripts describing new developments or important results of a preliminary nature. These Notes should not exceed 2500 words (where a figure or table counts as 200 words). Following informal review by the Editors, they may be published within a few months of the date of receipt. Style requirements are the same as for regular contributions (see inside back cover).

Calculation of High-Enthalpy Aerothermal Environment in an Arcjet Facility

Takeharu Sakai*
Nagoya University, Nagoya 464-8613, Japan
and
Toshiyuki Suzuki,† Kazuhisa Fujita,‡ and Takeshi Ito§
Japan Aerospace Exploration Agency, Tokyo 182-0012, Japan

DOI: 10.2514/1.26963

Nomenclature

c_i	=	mass fraction for species i
c_{p_i}	=	specific heat at constant pressure for species i, J/(kg · K)
H_{av}	=	mass-averaged enthalpy, J/kg
H_{cl}	=	centerline enthalpy, J/kg
h_i^0	=	enthalpy of formation for species i, J/kg
I	=	electrical current, A
$\dot{m}$	=	mass flow rate, kg/s
p_{ch}	=	chamber pressure, atm
T	=	temperature, K
U	=	velocity, m/s
V	=	voltage, V
η	=	heater thermal efficiency

I. Introduction

SEGMENTED-CONSTRICTOR type arc-heated wind tunnels are used to test the heat shield materials for spacecraft thermal protection systems. The arc-heated wind tunnel consists of an upstream electrode (anode) chamber, constrictor section, downstream electrode (cathode) chamber, and a diverging–converging nozzle connecting to a test chamber. In the test section, the heat shield materials are exposed to a high-enthalpy flow environment produced by the facility. The high-enthalpy environment is often such that the flow does not reach equilibrium condition at the edge of the boundary layer over the tested material. In such a case, we need to calculate the flow properties at the surface of the material using a computational fluid dynamics approach to understand the thermal response of the material [1]. For this purpose, the arcjet freestream conditions must be known accurately.

To calculate an arcjet freestream condition, two important physical processes occurring in the arcjet wind tunnel should be accounted for: the heating process in the arc heater region upstream of the nozzle throat and the relaxing process in the expanding nozzle region downstream of the nozzle throat. The ARCFLO3 code has been developed recently to calculate the flowfield in the segmented-constrictor type of arc heaters [2]. Unlike the arc heater flowfield code named ARCFLO developed in the 1970s [3], which is able to calculate the flow in the constrictor section, this new code calculates the flow from the anode chamber to the nozzle throat [2]. Arcjet freestream conditions can be calculated fully theoretically if a nonequilibrium expanding nozzle calculation is made with the calculated flow properties at the nozzle throat obtained by using the ARCFLO3 code. In addition, because the radial distribution of the flow properties at the nozzle throat is calculated with the ARCFLO3 code, the unified computational method can give the radial flow properties in the arcjet freestream at the test section.

We tried to make such a unified calculation very recently for one operating condition in an arcjet facility [1]. However, the question remains as to how well such a computational approach predicts the flow properties in an arcjet freestream. It is the purpose of the present work to test the validity of the unified method.

The method is applied to calculate the flowfield in a 0.75-MW arcjet wind-tunnel facility at the Institute of Aerospace Technology of the Japan Aerospace Exploration Agency (IAT/JAXA) in Japan. This facility was chosen for the following reasons:

1) In the recent measurement [4] in the IAT/JAXA arcjet facility, the operational characteristic parameters for a wide range of conditions were obtained. The experimental data offer an opportunity to test the current state of the computational modeling in the proposed method.

2) In our previous work, the ARCFLO3 code was applied for the arc heater flowfield calculation only in a high-power-level arc heater, such as the 20- or 60-MW arcjet facility at NASA Ames Research Center [2]. The applicability of the ARCFLO3 code to submegawatt class facilities is unknown.

II. Physical and Numerical Modeling

Two computational blocks are built to calculate an arcjet freestream: one block represents the entire flowfield in the arc heater section from the upstream electrode chamber to the nozzle throat and another represents the nozzle section downstream of the nozzle throat. A 180×40 grid is used for the arc heater section, and a 250×50 grid is used for the nozzle section. The diameter of the constrictor is 0.0254 m and the length is 0.39 m. The nozzle has a conical geometry with the throat diameter of 0.025 m. The half angle of the conical nozzle is 15 deg. The geometrical area ratio at the nozzle exit is 21. The test section is represented by an equivalent nozzle, which extends past the physical exit location, to calculate the flow properties at an axial location in the test chamber. The effective area ratio at the axial location was chosen to reproduce the pitot pressure values measured at the location.

The ARCFLO3 code is used to calculate the flowfield in the arc heater section. The code calculates an axisymmetric viscous flow, assuming thermochemical equilibrium therein. Mass, momentum, and total energy conservation equations are discretized using a finite

Received 1 August 2006; revision received 13 September 2006; accepted for publication 13 September 2006.

*Assistant Professor, Department of Aerospace Engineering. Member AIAA.
†Postdoctoral Fellow, Institute of Aerospace Technology. Member AIAA.
‡Senior Research Scientist, Institute of Aerospace Technology. Member AIAA.
§Head, High Enthalpy Flow Research Group, Institute of Aerospace Technology. Member AIAA.

volume method. Joule heating and radiative source terms are included in the right-hand side of the energy equation. An air model is used as the test gas, which consists of 11 chemical species (N, O, N_2, O_2, NO, N^+, O^+, N_2^+, O_2^+, NO^+, and e^-). Solutions are obtained by numerically integrating the equations in time to steady state. The code needs two operating parameters of an arcjet wind tunnel: mass flow rate and electrical current. The details of the numerical procedure in the ARCFLO3 code are given in [2].

In the expanding flow region beyond the throat, the axisymmetric viscous flow is assumed to be in thermochemical nonequilibrium. The air model has five chemical species (N, O, NO, N_2, and O_2). Because the total mass fraction of the ionized species in the throat region is less than 0.001, their contribution is negligible for the present purpose of the calculation. Species mass, momentum, vibronic energy, and total energy conservation equations are discretized using a finite volume method. A finite rate chemical reaction and vibrational relaxation source terms are included in the right-hand side of the species mass and vibronic energy equations, respectively. A thermochemistry model [5] is used for the expanding nozzle flow calculations. Solutions are obtained by integrating the equations in time. The inlet boundary condition at the entrance of the nozzle is given by the ARCFLO3 solutions at the throat. The nozzle wall is taken to be an isothermal wall of 500 K. The wall is assumed to be noncatalytic.

III. Results and Discussion

The IAT/JAXA arcjet wind tunnel was operated for the mass flow rates from 0.01 to 0.02 kg/s and the electrical currents from 300 to 700 A. Experimental measurements were made of arc current, voltage between electrodes, chamber pressure, heater thermal efficiency, and mass-averaged enthalpy for the operating conditions. The experimental error is 1% for the voltage and 0.1% for the chamber pressure, respectively. The mass-averaged enthalpies were determined by using the energy balance method [4]. The experimental error was estimated to be 10–20% for the heater efficiency and the mass-averaged enthalpy, respectively.

In the test section, the heat transfer rate to the stagnation point of a blunt body and stagnation point pressure were measured. The blunt body has a rounded flat disk shape with the diameter of 4.0 cm. A Gardon gauge heat flux sensor was used for the measurement. The sensor was placed at the stagnation point of the body. During the measurement, the Gardon gauge was water-cooled to maintain the sensor at constant temperature. The experimental error of the stagnation point heat flux is about 3%. A pitot pressure probe was used to measure the stagnation point pressure. The experimental error of the pitot pressure is 0.1%.

ARCFLO3 calculations are performed at five mass flow rates for three different electrical current conditions of 300 500, and 700 A for the IAT/JAXA arc heater. The sensitivity of the computational grid to the calculated flow properties is small. Calculation is carried out for the case of $I = 700$ A and $\dot{m} = 0.02$ kg/s by using a 220×80 grid for the arc heater section and a 300×100 grid for the nozzle section. The difference of the calculated flow properties between the two sets of the grid system was less than 1%.

The measured and the computed operational characteristic parameters for arc voltage, chamber pressure, heater efficiency, and mass-averaged enthalpy are presented in Figs. 1 and 2, respectively. In Fig. 1a, we see that the calculation tends to overestimate the measured voltages in the lower mass flow rates by 10–17% for all electrical current cases, but the difference between measurement and calculation becomes smaller as the mass flow rate increases. From Fig. 1b, the calculated chamber pressures are in a good agreement with the measurement over all mass flow rates and electrical currents considered. In Fig. 2a, the calculated heater efficiencies are lower than the measured ones at the lower mass flow rates by about 4–10% and are higher at the higher mass flow rates by about 5–10% for all electrical current cases. Finaly, as Fig. 2b shows, the calculation gives a better agreement with the measured mass-averaged enthalpy for the cases of $I = 500$ and 700 A. For the case of $I = 300$ A, the calculated results are slightly higher than the measurement by about

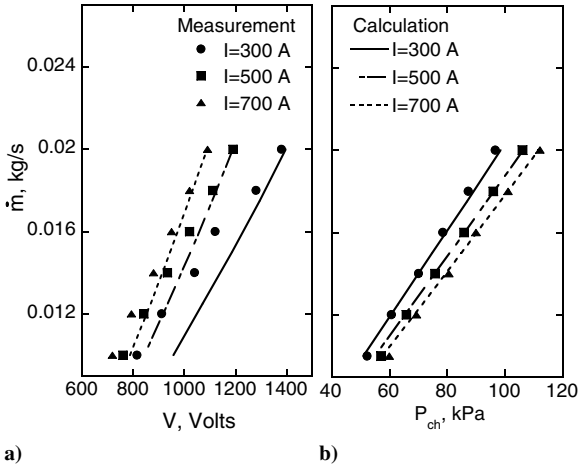

Fig. 1 Comparison of operational characteristic parameters between calculation and experiment: a) voltage and b) chamber pressure.

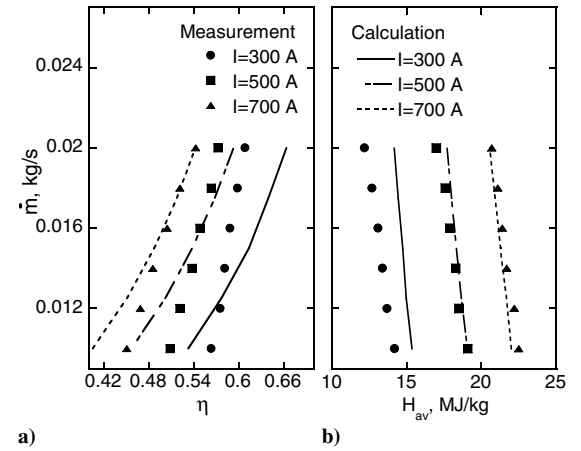

Fig. 2 Comparison of operational characteristic parameters between calculation and experiment: a) heater thermal efficiency and b) mass-averaged enthalpy.

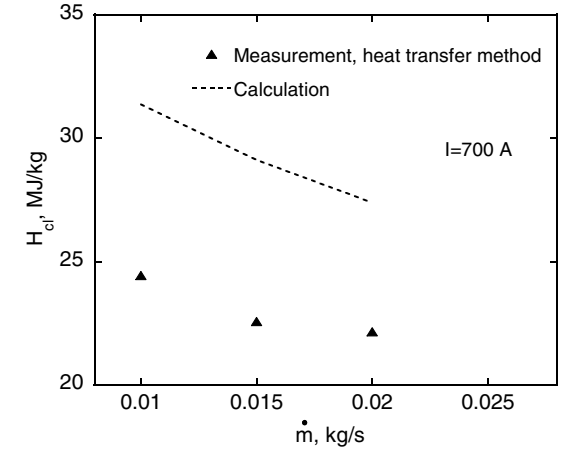

Fig. 3 Comparison of centerline enthalpy between calculation and experiment.

9–17%. The differences between the ARCFLO3 calculation and the measurement are roughly within the experimental errors.

In Fig. 3, centerline enthalpy is given against mass flow rate for the case of $I = 700$ A and the comparison of the centerline enthalpy is made between calculation and measurement. The measured values are deduced based on a heat transfer method. In this method, the centerline enthalpy is determined from the heat transfer rate to the

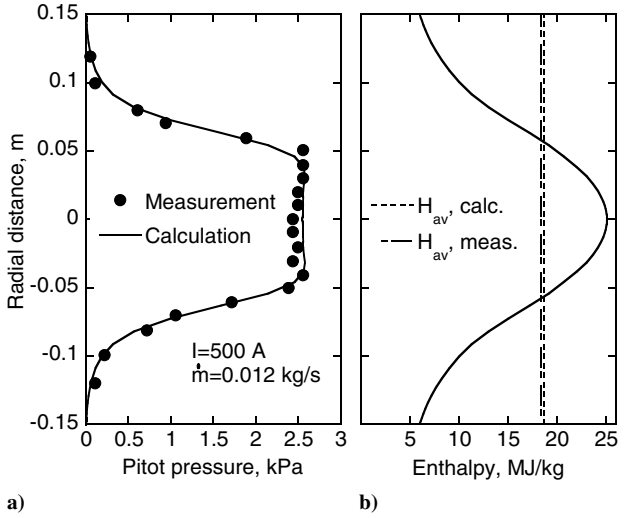

Fig. 4 Comparison of radial flow properties in arcjet freestream between calculation and experiment for the case of $I = 500$ A and $\dot{m} = 0.012$ kg/s: a) pitot pressure and b) enthalpy. Computed and measured mass-averaged enthalpy values are given in Fig. 4b.

stagnation point of a blunt body [6]. In the present analysis, so-called Fay–Riddell values are calculated using the formula given by Zoby [7]. The calculated centerline enthalpy value is given by

$$H_{\mathrm{cl}} = \sum_i c_i c_{p_i} T + \frac{U^2}{2} + \sum_i c_i h_i^0 + e_v$$

Each term of the enthalpy expression given in the right-hand side of this equation represents thermal, kinetic, chemical, and vibronic modes, respectively. The present calculations show that the chemical mode in the total enthalpy expression is 55 to 60% of the total enthalpy, the kinetic mode is 35 to 39%, and the sum of the thermal and vibronic modes are less than 5%. From the figure, the calculated centerline enthalpy values are higher than the measured ones by about 30%.

The discrepancy between measurement and calculation seen in Fig. 3 could be attributed to neglecting the possible catalytic efficiency of the surface on the Gardon gauge. The Gardon gauge is usually assumed to be fully catalytic. However, the catalytic efficiency could be reduced when it is in a dissociated flow regime. As was indicated from the large extent of the chemical mode in enthalpy shown earlier, the arcjet flow in the centerline region could contain a large amount of atomic species. In addition, atomic species can increase because dissociation reaction occurs behind the shock wave over the blunt body. Therefore, the flow environment over the blunt body is believed to be highly dissociated. Park et al. calculated the centerline enthalpy using the heat transfer method for a 60 MW arcjet facility. The results showed that the centerline enthalpy deduced by the heat transfer method was strongly affected by catalytic efficiency [6]. In the present measurement, the true value of the catalytic efficiency was unknown.

In Fig. 4a, the radial pitot pressure distribution is compared between measurement and calculation at the axial location of 0.1 m from the nozzle exit. The calculation is carried out for the case of $\dot{m} = 0.012$ kg/s and $I = 500$ A. In the core region for which the pitot pressure value is nearly constant, a good agreement is seen between the calculation and the measurement. It is found from the measurement that the diameter of the inviscid core region is about 0.1 m. Calculation replicates the measured pitot pressure profile fairly well.

Figure 4b shows the calculated total enthalpy distribution in the radial direction at the same axial location for the same case. The calculated and the measured mass-averaged enthalpy values are also given in the figure for the purpose of comparison. For the mass-averaged enthalpy, a good agreement is obtained between calculation and measurement. Unlike the pitot pressure profile, the total enthalpy distribution is found to be nonuniform. The enthalpy value is decreased by about 20% within the flow region for which the pitot pressure value is constant. The ratio of the centerline enthalpy to the mass-averaged enthalpy is 1.33 for this case. The calculations for other operating conditions show that the ratio of the centerline enthalpy to the mass-averaged enthalpy are varied from about 1.4 to 1.3 as mass flow rate increases. It should be noted that the diameter of the model tested in the IAT/JAXA arcjet facility is typically 0.04 m. The calculation predicts a roughly constant enthalpy distribution for the region impacting the face of the model, though the results are not shown here. At the time of the present work, no experimental data was available for comparison of the flow properties in the radial direction. A work is left for the future to examine the accuracy of calculated centerline enthalpy values.

IV. Conclusions

The present computational method can reproduce the existing experimental data taken in the IAT/JAXA arcjet wind tunnel. From the fair agreement of the operational characteristic data between measurement and calculation, it is found that ARCFLO3 code is able to calculate the arc heater flowfield in a submegawatt arcjet wind tunnel. By using the ARCFLO3 solution at the nozzle throat, the nozzle expanding flow calculation can replicate the measured inviscid core region fairly well. The computed centerline pitot pressure is also in good agreement with the data. The computed centerline enthalpy is higher than the measured one that was determined by a heat transfer method. More experimental data will be needed for the thorough validation of the present method.

Acknowledgment

The first author would like to thank Masahito Mizuno of the Institute of Aerospace Technology of the Japan Aerospace Exploration Agency (IAT/JAXA) for helpful discussions.

References

[1] Suzuki, T., Sakai., T., and Yamada, Y., "Calculation of Thermal Response of Ablator Under Arc-jet Flow Condition," *Journal of Thermophysics and Heat Transfer* (submitted for publication).

[2] Sakai, T., "Computational Simulation of High Enthalpy Arc Heater Flows," *Journal of Thermophysics and Heat Transfer* (to be published).

[3] Nicolet, W. E., Shepard, C. E., Clark, K. C., Balakrishnan, A., Kesselring, J. P., Suchsland, K. E., and Reese, J. J., "Analytical and Design Study for a High-Pressure, High-Enthalpy Constricted Arc Heater," Arnold Engineering Development Center Rept. TR-75-74, July 1975.

[4] Matsuzaki, T., Ishida, K., Watanabe, Y., Miho, K., Itagaki, H., and, Yoshinaka, T., "Construction and Characteristics of the 750 kW Arc Heated Wind Tunnel," National Aeronautical Laboratory, Rept. TM-760, Oct. 2002 (in Japanese).

[5] Gökçen, T., "Computation of Nonequilibrium Viscous Flows in Arc-Jet Wind Tunnel Nozzles," AIAA Paper 94-0254, 1994.

[6] Park, C., Raiche, D. M., Driver, D. M., Olejniczak, J., Terrazas-Salinas, I., Hightower, and Sakai, T., "Comparison of Enthalpy Determination Methods for an Arc-jet Facility," AIAA Paper 2004-487, 2004.

[7] Zoby, E. V., "Empirical Stagnation-Point Heat-Transfer Relation in Several Gas Mixtures at High Enthalpy Levels," NASA TN D-4799, Oct. 1968.